Naunyn-Schmiedeberg's Archives of Pharmacology
https://doi.org/10.1007/s00210-020-02021-x

ORIGINAL ARTICLE

Involvement of selective GABA-A receptor subtypes in amelioration of cisplatin-induced neuropathic pain by 2′-chloro-6-methyl flavone (2′-Cl-6MF)

Nasiara Karim[1] · Imran Khan[2] · Abeer Abdelhalim[3] · Sobia Ahsan Halim[4] · Ajmal Khan[4] · Nouman Altaf[1] · Waqar Ahmad[1] · Rukhsana Ghaffar[1] · Ahmed Al-Harrasi[4]

Received: 27 July 2020 / Accepted: 8 November 2020

Abstract

Cisplatin-induced peripheral neuropathic pain is a common adverse effect of chemotherapy. The present study evaluated the effects of 2'-chloro-6-methylflavone (2'-Cl-6MF) at recombinant α1β2γ2L, α2β1-3γ2L, and α3β1-3γ2L GABA-A receptor subtypes expressed in *Xenopus* oocytes and subsequently evaluated its effectiveness in cisplatin-induced neuropathic pain. The results showed that 2'-Cl-6MF potentiated GABA-elicited currents at α2β2/3γ2L and α3β2/3γ2L GABA-A receptor subtypes. The potentiation was blocked by the co-application of flumazenil (a benzodiazepine (BDZs) site antagonist). In behavioral studies, mechanical allodynia was induced by intraplantar injection of cisplatin (40 μg/paw) in Sprague Dawley rats, and behavioral assessments were made 24 h after injection. 2'-Cl-6MF (1, 10, 30, and 100 mg/kg, i.p.), was administered 1 h before behavioral evaluation. Administration of 2'-Cl-6MF (30 and 100 mg/kg, i.p) significantly enhanced the paw withdrawal threshold and decreased mechanical allodynia. The standard drugs, gabapentin (GBP) at the dose of 70 mg/kg, and HZ 166 (16 mg/kg), i.p. also significantly enhanced the paw withdrawal threshold in mechanical allodynia. Pretreatment with pentylenetetrazole (PTZ) (15 mg/kg, i.p.) and flumazenil reversed the antinociceptive effect of 2'-Cl-6MF in mechanical allodynia indicating GABAergic mechanisms. Moreover, the binding mechanism of 2'-Cl-6MF was rationalized by in silico modeling tools. The 3D-coordinates of α2β2γ2L and α2β3γ2L were generated after homology modeling of the α2 subtype and 2'-Cl-6MF was at predicted binding sites of the developed models. The α2 model was compared with the α1 and α3 subunits via structural and sequence alignment. Molecular docking depicted that the compound binds efficiently at the neuromodulator binding site of the receptors. The findings of this study revealed that 2'-Cl-6MF ameliorated the manifestations of cisplatin-induced neuropathic pain in rats. Furthermore, we also conclude that GABAergic mechanisms may contribute to the antinociceptive effect of 2'-Cl-6MF. The molecular docking studies also confirm the involvement of the BDZs site of GABA-A receptors. It was observed that Ile230 of α2 stabilize the chlorophenyl ring of 2'-Cl-6MF through hydrophobic interactions, which is replaced by Val203 in α1 subunit. However, the smaller side chain of Val203 does not provide hydrophobic interaction to the compound due to high conformational flexibility of α1 subunit.

Keywords Chemotherapy-induced neuropathic pain · Cisplatin · 2'-Chloro-6-methylflavone · Mechanical allodynia · Gabapentin · GABAergic

✉ Nasiara Karim
nasiara.karim@uom.edu.pk

[1] Department of Pharmacy, University of Malakand, Chakdara, Dir (Lower), KPK, Pakistan

[2] Department of Pharmacy, University of Swabi, Swabi, KPK, Pakistan

[3] Chemistry Department, Faculty of Science, Taibah University, Al-Madinah Al-Munawarah 30002, Saudi Arabia

[4] Natural and Medical Sciences Research Center, University of Nizwa, Birkat Al Mauz, 616 Nizwa, Oman

Introduction

Chemotherapy-induced neuropathic pain occurs as a result of chemotherapy in 7–8% of the affected population and may be severe in 5% of cases (Bouhassira et al. 2008). The most common antineoplastic drugs associated with chemotherapy-induced neuropathic pain include cisplatin, paclitaxel, and vinca alkaloids. Almost 30–40% of patients treated with these drugs develop serious neuropathic pain.

Cisplatin is a platinum-based compound used in combination with other chemotherapeutic agents in the treatment of

Published online: 22 November 2020

solid tumors (Deuis et al. 2014). Cisplatin is typically used to treat neck, head, lung, ovarian, and testicular tumors. Cisplatin-induced peripheral neuropathy is usually dose-dependent and occurs at a dose greater than 300 mg/m^2 (Krarup-Hansen et al. 1993). This kind of chronic neuropathic pain usually affects upper and lower limbs and causes symptoms including dysesthesias and paresthesias (Roelofs et al. 1984; Thompson et al. 1984). Morphological and electrophysiological studies have shown that cisplatin-induced peripheral neuropathy largely affects sensory neurons (Thompson et al. 1984). Cisplatin-induced peripheral neuropathy usually persists for months and years even after the cessation of therapy and is believed to be due to the accumulation of platinum-based agents in the dorsal root ganglia (Gregg et al. 1992).

Chemotherapy-induced neuropathic pain thus prevents patients from completing their duration of treatment with life-saving drugs leading to noncompliance or prevents prolonging treatment they need. The treatment of chemotherapy-induced neuropathic pain is difficult and often accompanied by serious adverse effects (Park 2014). Therefore, the development of effective and inexpensive and selective novel drugs to be effective as analgesics in chemotherapy-induced peripheral neuropathy is of utmost importance.

Several pathophysiological mechanisms including oxidative stress, activation of apoptotic pathways, changes in calcium homeostasis, myelinated and unmyelinated fibers loss, and increased ion channel expression and activity have been implicated in chemotherapy-induced neuropathic pain (Quintão et al. 2019). Antidepressants drugs such as duloxetine have been found useful to alleviate this pain (Smith et al. 2013). Other drugs that are usually used to treat these pain conditions include anticonvulsant drugs that modulate or block voltage-gated Na + or Ca2+ channels (Sang and Hayes 2006). Other anticonvulsive drugs such as benzodiazepine site agonists, which enhance neuronal inhibition through positive modulation of GABA-A receptor–mediated neurotransmission are also effective. Reduced GABAergic or glycinergic inhibition in the spinal dorsal horn (i.e., in the sensory part of the spinal cord) is a major contributor to chronic pain syndromes (Coull et al. 2003; Harvey et al. 2004), suggesting that drugs that facilitate spinal inhibition might be useful to treat chronic neuropathic pain. Thus in line with this concept, previous work has shown that spinal injection of benzodiazepine site agonists provides pain relief in several rodent models of neuropathic pain and inflammation (Knabl et al. 2008).

Mammalian GABA-A receptors are heteropentameric ion channels assembled from a repertoire of 19 subunits. The most common subtypes of GABA-A receptors contain two α-, two β- and one γ2-subunits. Pharmacological properties of the different GABA-A receptor subtypes are best characterized by the type of α-subunit present in the individual receptors (Olsen and Sieghart 2008). Experiments in genetically modified mice demonstrated a particular relevance of GABA-A receptors with α2-type benzodiazepine pharmacology (α2-GABA$_A$Rs) for analgesic effects mediated by spinally applied benzodiazepines (Knabl et al. 2008). These and subsequent experiments (Knabl et al. 2009) have shown that the analgesic actions of benzodiazepines site agonists occur independently from their sedative action, which is mediated by the α1-GABA-A receptor subtype (Rudolph et al. 1999). Thus, the identification of selective α2-GABA-A receptor subtype agonists will provide leads for the development of novel and effective analgesics.

Our discovery that flavonoids distinctly modulate/directly activate GABA-A receptors identifies lead molecules and a novel mechanism of channel modulation that could provide society with effective adjunct or alternative analgesics to be effective in chemotherapy-induced neuropathic pain that has reduced side-effects compared to current therapies. Since we have shown that selected flavonoids have enhanced efficacy at α2-containing GABA-A receptors (Karim et al. 2011), thus it is anticipated that flavonoids with selectivity towards α2-GABA-A receptor subtype will be effective in alleviating neuropathic pain associated with chemotherapy. Thus, we sought to investigate 2'-Cl-6MF (Fig. 1) using electrophysiological and in vivo studies for its effectiveness in cisplatin-induced neuropathic pain.

Materials and methods

Cisplatin, gabapentin, morphine sulfate, PTZ, flumazenil, HZ 166, DMSO, and normal saline were purchased from Sigma Aldrich, whereas naloxone (98%) was purchased from Hangzhou Uniwise International Co., Ltd., China. Reagents were also purchased from Aldrich Chemical Co. Ltd. (St Louis, MO) and were of analytical grades. Human α1, α2, β2, and γ2L DNA in pcDM8 were provided by Dr. Paul Whiting (Merck, Sharpe and Dohme Research Labs, Harlow, UK), α3 and β3 in pGEMHE, and β1 in PCDM8 were a gift from Dr. Bjarke Ebert (H. Lundbeck A/S, Valby, Denmark).

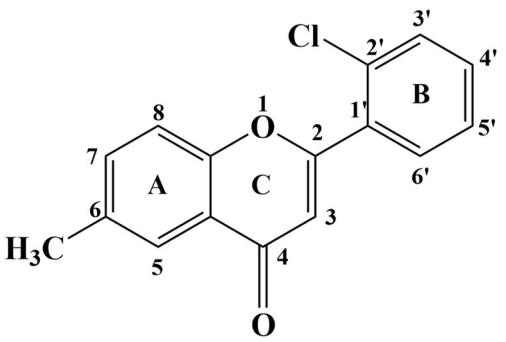

Fig. 1 Structure of 2'-chloro-6-methylflavone

Synthesis of 2′-chloro-6-methylflavone

Thin-layer chromatography was performed on pre-coated silica gel (0.2 mm, $60F_{254}$), Spots were visualized under ultraviolet light at 254, alkaline potassium permanganate solution (0.5% w/v), and iodine vapors. Column chromatography was performed on silica gel 60 (Merck). High-resolution ESI mass spectra were registered on Bruker Bio Apex II 7 T instrument (Bruker Daltonics).^{1}H NMR spectra were recorded at 400 MHz using a Varian (Palo Alto, CA) Gemini 400 spectrometer. The chemical shift values are presented in ppm (δ) relative to tetramethylsilane (TMS) as an internal standard and the coupling constant (*J*) is in Hertz.. ^{13}C NMR spectra were recorded at 100.5 MHz using a Varian (USA) 400 MI spectrometer. The chemical shift values are presented in ppm (δ).

Butyllithium (33.45 mmol) was added under nitrogen atmosphere to a solution of diisopropylamine (34.96 mmol) in THF (25 mL) at − 78 °C and was stirred for 10 min then the solution temperature was raised to 0 °C for 10 min then it was cooled back to − 78 °C. A solution of 2-hydroxy-5-methyl acetophenone **(1)** (16.65 mmol) in THF (50 mL) was added and the solution was stirred for 2 h at −78 °C followed by the addition of solution of 2-chlorobenzoyl chloride **(2)** (16.79 mmol) in THF (50 mL) and the resulting solution was stirred at room temperature for 36 h. The reaction was quenched by the addition of saturated ammonium chloride solution. The resulting mixture was then extracted with dichloromethane and was washed with brine and dried using sodium sulfate to produce 1-(2-hydroxy-5-methylphenyl)-3-(2-chlorophenyl)propane-1,3-dione **(3)**. Purification was achieved by silica gel column chromatography (hexane: EtOAc, 8:2). The resulted compound (**3**) (3.5 mmol) was added to glacial acetic acid (7 mL) and was refluxed with sulfuric acid (7 mmol) for 16 h at 120 °C.

The reaction mixture was concentrated under reduced pressure. The crude product was purified by silica gel column chromatography (hexane: EtOAc, 4:6) and recrystallized using acetone to afford pure 2′-chloro-6-methylflavone **(4)**.

2′-Chloro-6-methylflavone **(4)**: ^{1}H-NMR (DMSO-d_6, 400 MHz) δ ppm: 7.78 (1H, dd, J = 7.9, 1.4 Hz), 7.82 (m, 1H), 7.63 (1H, dd, J = 8.2, 7.4 Hz), 7.53 (1H, dd, J = 1.6, 0.5 Hz), 7.45 (1H, dd, J = 8.2, 1.2 Hz), 7.34 (1H, dd, J = 7.9, 7.4 Hz), 7.11 (1H, dd, J = 8.3, 0.5 Hz), 6.95 (1H, dd, J = 8.3, 1.6 Hz), 6.56 (1H, s), 2.35 (3H, s). ^{13}C-NMR (DMSO-d_6, 100.5 MHz) δ ppm: 177.65, 159.70, 154.2, 134.02, 133.94, 130.72, 130.60, 130.56, 128.33, 128.15, 127.33, 124.62, 123.43, 118.78, 105.61, 20.90. MS (ESI) m/z = 271.1 [M + 1]. HRMS (ESI) calcd for $C_{16}H_{11}O_2Cl$ [M^+ + H] 271.0526, found 271.0527 (Scheme 1).

Expression of recombinant GABA receptors in *Xenopus* oocytes

Oocyte preparation

Sexually mature female *Xenopus laevis* were maintained under optimal conditions by authorized animal keepers at The University of Sydney Animal House and fed standard frog food. Stage V–VI oocytes were harvested under 0.1% tricaine (3-aminobenzoic acid ethyl ester) anesthesia. Oocytes were defolliculated by shaking for approximately 1 h at 18 °C in collagenase (2 mg/mL) dissolved in OR2 solution containing (in mmol/L): NaCl 96; KCl 2; CaCl2 1, MgCl2 1; HEPES 5, pH 7.4. cDNA vectors were linearized with the appropriate restriction endonucleases and capped transcripts were produced from linearized plasmids using the 'mMessage mMachine' T7 transcript kit from Ambion (Austin, TX, USA).

Stage V–VI oocytes were sorted and injected (Nanoject, Drummond Scientific Co., Broomali, PA) with cRNA reconstituted in nuclease-free water in a ratio of 1α (25 ng): 1β (25 ng): 5 (γ) (125 ng). Oocytes were incubated for up to 4–8 days in standard ND96, pH 7.4, supplemented with pyruvate (2.5 mM), theophylline (0.5 mM), gentamycin (50 μg /mL), and 2% horse serum at 18 °C.

Electrophysiology

Currents were recorded using the two-electrode voltage-clamp technique according to our previously described method (Karim et al. 2011). Glass microelectrodes were filled with 3 M KCl (0.5–2 MΩ). Oocytes were clamped at − 60 mV and continuously perfused with ND96 solution (96 mM NaCl, 2 mM KCl, 1 mM $MgCl_2$, 1.8 mM $CaCl_2$, 5 mM HEPES, pH 7.5). Current amplitudes were calculated using Chart program version 5 (ADInstruments, NSW, Australia). Responses to GABA applications were normalized as $I\%$ = (I/Imax) × 100, where I is the peak amplitude of current response and Imax is the maximum current produced by GABA measured from individual cells. The enhancement of GABA-

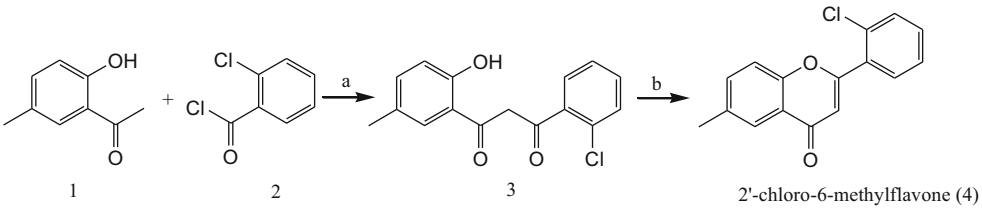

Scheme 1 Synthesis of 2′-choloro-6-methylflavone. **a** butyllithium, diisopropylamine, 2 h at − 78 °C; **b** Glac. AcOH, conc H_2SO_4, 16 h at 120 °C

induced currents was tested by coapplying increasing concentrations of the drugs with a specific concentration of GABA that produced approximately 10% of maximal activation. EC10 was determined from the GABA dose-response curve, constructed from 6 to 10 cells and calculated as the concentration that produced 10% current of the maximum response (current) produced by GABA. Current responses were normalized as % potentiation = ((Idrug+GABA-IGABA)/IGABA)100, where Idrug+GABA is the control GABA current in the presence of a given concentration of a drug, and IGABA is the amplitude of the control GABA current alone.

Animals

Sprague Dawley rats of either sex (50% male; 50% female) in the weight range of 150–220 g were purchased from the Department of Pharmacy, the University of Peshawar for breeding purposes. The animal colony was established and maintained in the animal house of the University of Malakand. The animals had access to freshwater and standard chow food ad libitum. The animals were maintained at 12 h light and dark cycle and with room temperature maintained at 22–25 °C. All experimental procedures involving animals were approved by the Animal Ethical Committee of the Department of Pharmacy, University of Malakand (DAEC/PHARM/2016/15), and were conducted according to the guidelines of the UK animal scientific procedure act, 1986.

Cisplatin-induced neuropathic pain

A single-dose of cisplatin (0.4 μg, 4 μg, or 40 μg) was administered by 22 G shallow subcutaneous (s.c.) injection to the left hind paw (intraplantar injection) under 3% isoflurane anesthesia. This caused rapid induction of neuropathy which was evident within 1 h of injection (Deuis et al. 2014) and lasted for several days (8 days). No adverse effects including redness, swelling, or ulceration, were observed at the site of injection.

Assessment of nociceptive thresholds

Thermal and mechanical allodynia were used for assessing the pain threshold. Thermal allodynia was assessed using both hot and cold temperatures.

1. Cold allodynia: Cold allodynia was performed according to the modified acetone method previously described (Deng et al. 2012). Rats were placed underneath inverted plastic cages on an elevated metal mesh table. After habituation, an acetone bubble that formed at the end of a blunt (1 c.c.) insulin syringe was gently presented to the plantar surface of the hind paw. Acetone was applied to the paws 5 times with a 3-min interval. The animals were observed for 20 s after the application of acetone. The number of paw lifts, licks, and flinches was recorded over 5 min.
2. Hot plate test: Hot plate test was used to determine the effects of test compounds on cisplatin-induced neuropathic pain. This test was conducted according to the method previously described (Deuis et al. 2014; Miri et al. 2015). Heat allodynia was quantified by counting the number of paw lifts, shakes, or flinches over 5 min at 42 °C using a hot plate (HotPlate, IITC).
3. Mechanical allodynia: Mechanical allodynia was assessed using a digital Von Frey anesthesiometer. The paw withdrawal threshold (PWT) was assessed using a digital von Frey (Von Frey anesthesiometer equipped with a rigid tip (IITC Life Science, Woodland Hills, CA, USA). Rats were placed underneath inverted plastic cages and were positioned on an elevated mesh platform. Rats were allowed to habituate to the chamber for 10 min before testing. Stimulation to the hind paw plantar region was applied through the floor of a mesh platform. Mechanical stimulation was terminated upon paw withdrawal. Cisplatin-induced decreases in mechanical paw withdrawal were therefore defined as mechanical allodynia (Rahn et al. 2008). The endpoint was confirmed as paw withdrawal accompanied by head-turning, biting, and/or paw licking. The required pressure was indicated in grams and was considered to be the value of the paw withdrawal threshold (PWT). Each rat was tested three times, and the averages were considered to be the final results. Behavioral assessment was done 24 h after cisplatin injection. All behavioral experiments were performed in a blind fashion.

Drug administration

The effect of 2'-Cl-6MF and other compounds was assessed 24 h after administration of the cisplatin. Group I animals received only the normal diet with 0.9% NaCl alone and the animals in groups II–VIII animals received cisplatin in saline to a stock solution of 100 μg/10 ml. After 24 h, group III received GBP (75 mg/kg), and group IV received HZ 166 (16 mg/kg). From groups V to VIII, animals were administered a single i.p. injection of 2'-Cl-6MF (1, 10, 30, and 100 mg/kg, i.p.). All the test compounds were administered 1 h before behavioral assessment. The involvement of GABA-A receptors in the antiallodynic effect was assessed using various antagonists including PTZ (15 mg/kg, i.p.) and flumazenil (1 mg/kg, i.p.) which were administered 15 min before GBP (75 mg/kg), HZ 166 (16 mg/kg) or 2'-Cl-6MF (30 and 100 mg/kg, i.p.) administration. Naloxone (1 mg/kg, i.p.) was administered 15 min prior to morphine (5 mg/kg, i.p.) or 2'-Cl-6MF (100 mg/kg, i.p.) administration.

PTZ, gabapentin, HZ 166, morphine, naloxone, and flumazenil were dissolved in 0.9% saline whereas 2'-Cl-6MF was dissolved in a vehicle consisting of normal saline (95%), Tween 80 (4%), and DMSO (1%) and were administered in a total volume of 10 ml/kg body weight except morphine and naloxone which were administered in volume of 2 ml/kg body weight.

Computational modeling

Homology modeling and molecular docking

The binding mechanism of 2'-chloro-6-methylflavone was studied by computational tools including homology modeling and molecular docking. The 3D-complex of α2β2γ2L was generated by superimposing the $GABA_AR$α2 model on human $GABA_AR$α1 (present in $GABA_AR$α1β2γ2, PDB ID: 6D6T). The α2β3γ2L complex was generated by replacing α1 and β2 subtypes (present in 6D6T) with the $GABA_A$α2 model and β3 coordinates (taken from $GABA_A$α5β3 subtype, PDB code: 6A96) in $GABA_AR$α1β2γ2 (6D6T) The complexes were created in pentameric form.

The three-dimensional (3D-) structure of the $GABA_A$α2 subunit was built by homology modeling using a sequence of $GABA_A$α2 from the UniProtKB database (ID: P47869) (Supporting Information, Table S1). Human $GABA_AR$α1β2γ2 structure is present in a complex with GABA and drug flumazenil (PDB code: 6D6T). The percent (%) identity between $GABA_AR$α1 and $GABA_AR$α2 is 87%, therefore $GABA_AR$α1 was used as a template for modeling of α2 subunit by SwissModel server (https://swissmodel.expasy.org/). Model-Template sequence alignment is presented in Fig. S1 (Supporting Information). The quality and the stereochemical properties of the developed model were assessed by the Ramachandran plot (http://servicesn.mbi.ucla.edu/PROCHECK/) (Fig. S2). The neurotransmitter (GABA) binding site of $GABA_AR$α2 was inferred by multiple structural alignment of the model with the structures of human $GABA_A$α1β2γ2 (PDB codes: 6D6T and 6CDU) and mouse $GABA_A$α1 (PDB codes: 5OSB and 5OSC). For structure comparison of α2 subunit with α1 and α3 subunits, the coordinates of α3 were taken from SwissModel repository of models (https://swissmodel.expasy.org/repository/uniprot/P34903) with accession number P34903 (GBRA3_HUMAN). Subsequently, in silico molecular docking was carried out by Molecular Operating Environment (MOE version 2009.14). For docking, Hydrogen atoms were added on proteins, and partial charges were applied (based on MMFF94x force field). The structure of the ligand was generated and minimized by MOE (with MMFF94x force field, RMS gradient = 0.1 kcal/mol/Å). During minimization, MOE automatically adds hydrogen atom and partial charges on the ligand. Triangle Matcher docking algorithm and London dG scoring function were applied in docking. Results were analyzed by UCSF-Chimera (https://www.cgl.ucsf.edu/chimera/).

Statistical analysis

The data were expressed as mean ± SEM. Data were analyzed by unpaired *t* test for the comparison of two groups and ANOVA followed by Tukey's post hoc test for more than two groups. A *P* value less than 0.05 was considered statistically significant.

Results

Effect of 2′-Cl-6MF at α1β2γ2L and α2/3β1-3γ2L $GABA_A$ receptors

2'-Cl-6MF did not enhance the response to 10 μM GABA at α1-subunit-containing receptors (Fig. 2). The figure shows a sample current trace at α1β2γ2L receptors that indicate that coapplication of 100 μM with 10 μM did not enhance GABA-elicited currents (Fig. 2a). In contrast, 2'-Cl-6MF enhanced GABA-elicited currents at α2β2γ2L GABA-A receptors. 2'-Cl-6MF at 100 μM caused a 4.5-fold increase in the GABA EC10 response (Fig. 2b). 2'-Cl-6MF also enhanced the response to 10 μM GABA at α2β3γ2L but has no effect at α2β1γ2L receptors. The concentration-response curves of 2'-Cl-6MF in the presence of GABA EC10 response shows that maximum potentiation of $GABA_{EC10}$ induced currents was 449 ± 31 and 356 ± 22% at α2β2γ2L and α2β3γ2L receptors (Fig. 2c; Supplemental 2). 2'-Cl-6MF was also evaluated for possible potentiating effects of GABA at α3β1-3γ2L subtypes. 2'-Cl-6MF also caused moderate enhancement of GABA-elicited currents at α3β2/3γ2L subtype, but no increase was observed at α2β1γ2L receptors (Fig. 3 a and b). The concentration response curves of 2'-Cl-6MF in the presence of GABA EC10 indicated that maximum potentiation of 252 ± 35% at α2β2γ2L and 260 ± 45% (Fig. 3c; Supplemental 3).To investigate the involvement of classical high-affinity BDZ site on the potentiation of GABA-induced currents (10 μM) by 2'-Cl-6MF (30 μM), flumazenil (0.1, 1, and 10 μM) was coapplied. Flumazenil reduced GABA-induced currents at α2β2γ2L receptors in a concentration-dependent manner, with 10 μM blocking the response completely, indicating that 2'-Cl-6MF (30 μM) enhanced GABA-elicited currents via the classical BDZ binding site on GABA-A receptors (Fig. 2d).

Cisplatin-induced thermal allodynia

Intraplantar administration of cisplatin (40 μg/paw) did not induce thermal allodynia as it did not cause any observable

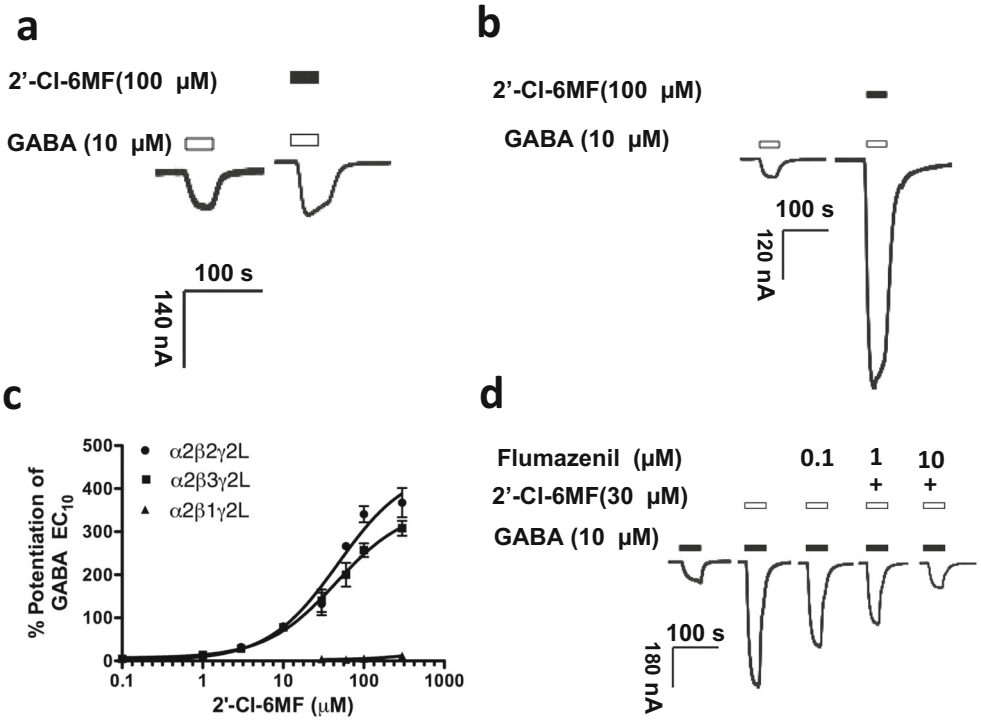

Fig. 2 2'-C-l6MF acted as positive allosteric modulators of α1/2- subunit-containing GABA-A receptors. **a** Current trace showing the effect of GABA (EC10: 10 μM) by 2'-Cl-6MF (100 μM) at human recombinant α1β2γ2L GABA-A receptors. **b** Sample current trace showing the effect of GABA (EC10: 10 μM) by 2'-Cl-6MF (100 μM) at human recombinant α2β2γ2L GABA-A receptors. **c** Concentration-response curves for 2'-Cl6MF in the presence of GABA (EC10 = 10 μM) at recombinant α2β2γ2L (●), α2β3γ2L (▲), and α2β1γ2L (♦) receptor subtypes. **d** Effect of flumazenil (Flu) on the potentiation of GABA-induced currents by 2'-Cl-6MF (30 μM) at human recombinant α2β2γ2L GABA-A receptors. Data are mean ± SEM (n = 3–6 oocytes)

changes in the number of paw lifts, shakes, or flinches. This observation is consistent with previous studies (Deuis et al. 2014) and clinical observation (data not shown).

Cisplatin-induced mechanical allodynia

Figure 4 shows the effects of intraplantar injection of cisplatin on the paw withdrawal threshold to mechanical stimulation. Panel A shows that a single injection of cisplatin 40 μg/paw caused a significant decrease in paw withdrawal threshold over 3 days (*$p < 0.05$, ***$p < 0.001$; Student t test (unpaired) that lasted for several days (data not shown). Panel B shows the cisplatin dose-dependently caused a significant decrease in paw withdrawal threshold at the doses of 0.4–40 μg/paw after 24 h (**$p < 0.05$, ***$p < 0.001$. One way ANOVA followed by Tukey's post hoc test).

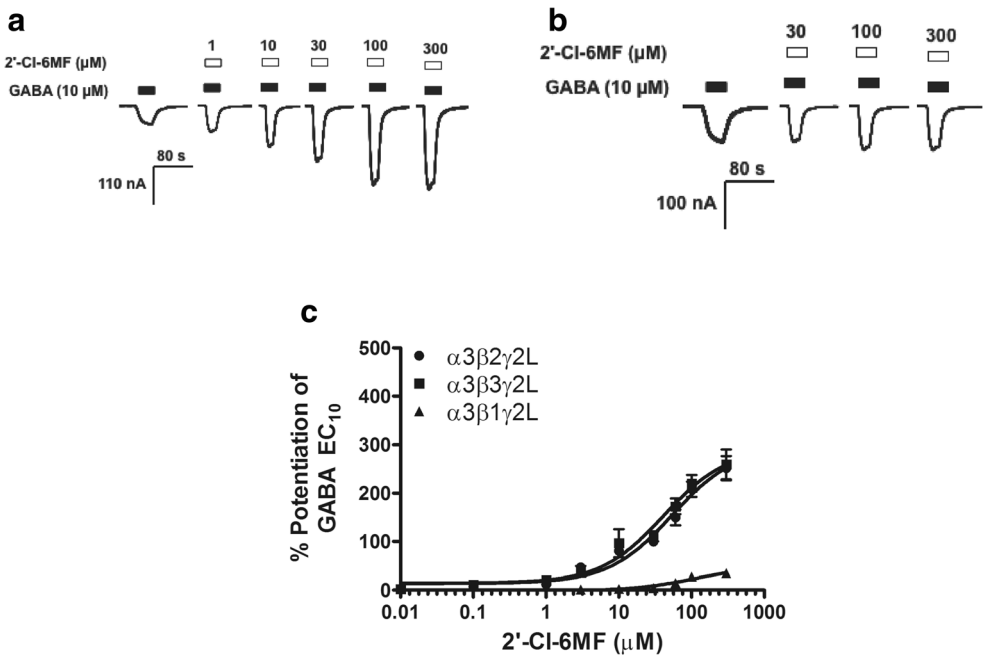

Fig. 3 Effect of 2'-C-l6MF on α3-subunit-containing GABA-A receptors. **a** Current trace showing the effect of GABA (EC10: 10 μM) by 2'-Cl-6MF (100 μM) at human recombinant α3β2γ2L GABA-A receptors. **b** Sample Current trace showing the effect of GABA (EC10: 10 μM) by 2'-Cl-6MF (100 μM) at human recombinant α3β1γ2L GABA-A receptors. **c** Concentration-response curves for 2'-Cl6MF in the presence of GABA (EC10 = 10 μM) at recombinant α3β2γ2L (●), α2β3γ2L (▲) and α2β1γ2L (♦) receptor subtypes. Data are mean ± SEM (n = 3–6 oocytes)

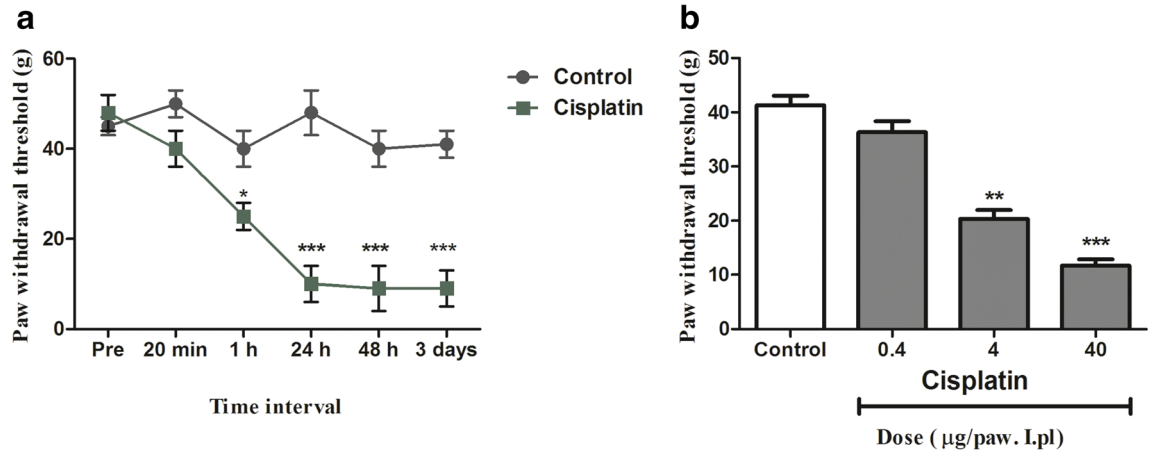

Fig. 4 An animal model of chemotherapy-induced neuropathy based on the intraplantar injection of cisplatin. **a** Intraplantar injection of cisplatin 40 µg significantly reduced paw withdrawal threshold to mechanical stimulation via Von Frey rigid filament compared to control (0.9% saline).*$p < 0.05$,***$p < 0.001$ compared with control. Data were analyzed by Student *t* test (unpaired). **b** A single intraplantar injection of cisplatin (0.4–40 µg/paw) caused mechanical allodynia dose-dependently (data shown at 24 h). **$p < 0.01$; ***$p < 0.001$ compared with control (one way ANOVA followed by Tukey's post hoc test). Data are expressed as mean ± SEM, $n = 8$ rats/group

Antinociceptive effect of 2'-Cl-6MF on cisplatin-induced mechanical allodynia

Figure 5 depicts the effect of 2'-Cl-6MF on cisplatin-evoked mechanical allodynia. Administration of cisplatin (40 µg/paw) caused a significant decrease in paw withdrawal threshold after 24 h compared to control ($F(6, 35) = 43.30$, ***$p < 0.001$). Administration of animals with 2'-Cl-6MF, GBP or HZ 166 significantly increased the paw withdrawal threshold in cisplatin-induced mechanical allodynia compared to cisplatin ($F(6, 35) = 43.30$, $^{###}p < 0.001$). 2'-Cl-6MF dose-dependently reversed cisplatin-induced reduction in paw withdrawal threshold at 10, 30, and 100 mg/kg, i.p. ($^{#}p < 0.05$, $^{##}p < 0.01$) compared to cisplatin group. No significant reduction in paw withdrawal threshold was observed with 2'-Cl-6MF at 1 and 10 mg/kg. GBP, administered as a reference drug, also significantly reversed cisplatin-induced mechanical allodynia at 70 mg/kg ($^{###}p < 0.001$).

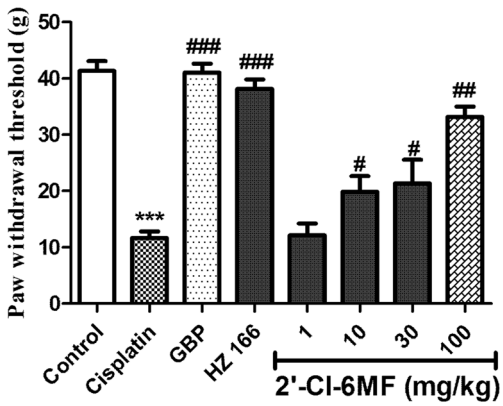

Fig. 5 Antiallodynic effect of 2'-Cl-6MF in cisplatin-induced mechanical allodynia at 24 h. ***$p < 0.001$ compared with control. $^{#}p < 0.05$, $^{##}p < 0.01$, compared to cisplatin group. Data are presented as mean ± SEM, $n = 8$. Statistical significance was determined using one way ANOVA followed by Tukey's post hoc test

Elucidation of the mechanism of action

To assess the involvement of GABAergic mechanisms in the antiallodynic effect of 2'-Cl-6MF, PTZ (15 mg/kg, i.p.) was administered 15 min before GBP (70 mg/kg), HZ 166 (16 mg/kg), and 2'-Cl-6MF (30 and 100 mg/kg) administration (Fig. 6). The results showed that both PTZ and flumazenil reversed the increases in paw withdrawal threshold (g) caused by 2'-Cl-6MF indicating the involvement of GABA-A receptors. A similar reversal of the antiallodynic effect of HZ 166 (16 mg/kg) was observed with flumazenil (3 mg/kg, i.p.) pretreatment. In contrast, PTZ did not inhibit GBP-induced enhancement of paw withdrawal threshold indicating that the antiallodynic effect of GBP is mediated by GABAergic mechanisms but does not involve GABA-A receptors. Furthermore, to rule out the role of opioid receptors in the antinociceptive effect of 2'-Cl-6MF, animals administered with either 2'-Cl-6MF (100 mg/kg, i.p.) or morphine (5 mg/kg, i.p.) were pretreated with NLX (1 mg/kg, i.p.). Pretreatment with NLX completely abolished the antinociceptive effect of morphine. In contrast, NLX did not inhibit the antinociceptive effect of 2'-Cl-6MF (100 mg/kg, i.p.) ruling out the involvement of opioid receptors (Fig. 6b).

Homology modeling and molecular modeling

Homology modeling was employed to generate the 3D-coordinates of α2 subunit to constitute α2β2γ2L and α2β3γ2L complexes. The developed models were used in molecular docking studies. The structure of human $GABA_A$ α1β2γ2 (PDB code: 6D6T) was used as a template to

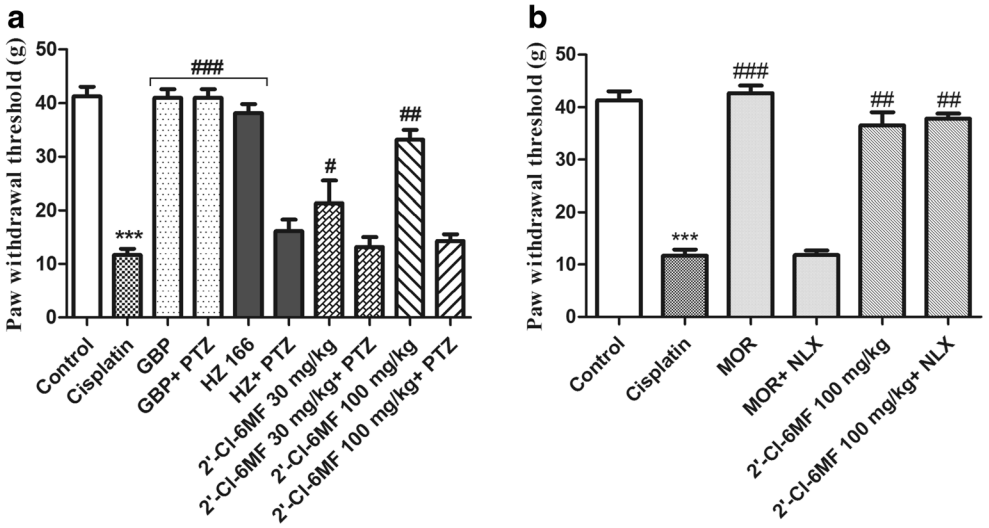

Fig. 6 Effect of PTZ (15 mg/kg, i.p.) on the antiallodynic effect of GBP or 2'-Cl-6MF and flumazenil (Flu) on HZ 166 (16 mg/kg, i.p.) or 2'-Cl-6MF (**a**); or effect of NLX (1 mg/kg, i.p.) on the antiallodynic effect of MOR (5 mg/kg, i.p.) or 2'-Cl-6MF (100 mg/kg) (**b**) in mechanical allodynia at 24 h using digital Von Frey anethesiometer. $^{***}p < 0.001$ compared with control. $^{\#}p < 0.05$, $^{\#\#}p < 0.01$, $^{\#\#\#}p < 0.001$ compared to cisplatin group. Data are presented as mean ± SEM, $n = 8$. Statistical significance was determined using one way ANOVA followed by Tukey's post hoc test

construct the model of $GABA_A$ α2. The percent (%) identity between template and model was 87% with 78% query coverage, and 0.0 E-value (Table S2). Moreover, $GABA_A$α2 possesses 87% and 85% identities with $GABA_A$α1 and $GABA_A$α5, respectively. The structural topologies of the template and α2 model were similar. The α2 model possesses 407 residues with an extracellular domain (ECD, residues 38–252), four transmembrane regions so-called M1 to M4, and an intracellular domain (ICD). M1 is composed of twenty residues (from 253 to 273) which are connected with M2 (of eighteen residues, 282–300) via loop region (274–281). M2 faces the ion channel and is linked with an extracellular loop (301–311) which connects M2 and M3 (312–337), whereas M3 and M4 (344–372) are connected through an ICD which is composed of 72 residues (340–412). This ICD region was stripped off from the model to align the coordinates of the model on the structure of the template. A signatory Cys-loop is located at the ECD constituted by an amino-terminal α-helix and ten β-strands folded into a β-sandwich. The neurotransmitter (GABA) binds at ECD between the α2-β2 interface while benzodiazepines (BZD) and allosteric modulator (flumazenil) bind at the α2-ɣ2 interface. Several other modulators including pregnenolone sulfate, alphaxalone, and THDOC bind at M2–M4 and M1–M4 regions of α2, respectively. The GABA binding site at the β2 subunit is composed of Tyr97, Tyr157, Phe200, and Tyr205 which stabilize the NH_3 group of GABA via π-cation interactions. The side-chain carboxylate group of Glu155 and Thr202 interacted with the amino nitrogen and carboxylate group of GABA, respectively through ionic interaction and hydrogen bond. The binding residues of α1 and α2 subunits are completely identical. The GABA binding site at α1 is constituted by Phe65, Arg67, Leu118, Leu128, and Thr130 which are identical to Phe92, Arg94, Leu145, Leu155, and Thr157 of the α2 subunit. Similar to Phe65(α1), Phe92(α2) forms the floor of the binding pocket and offers hydrophobic interactions, whereas side-chain guanidinium moiety of Arg94(α2) facilitates electrostatic interactions with the carboxylate group of GABA. Therefore, Phe92 and Arg94 of the α2 subunit play a crucial role in the binding of the substrate molecule. The benzodiazepine (BZD) binds at ECD of α2 which is composed of Phe127, His129, Ser186, Tyr187, Ala188, Ile230, Ser232, Ser233, Thr234, Tyr237, and Val239, this ECD faces α2–γ2 interface. These residues of α2 are identical to the Phe100, His102, Ser159, Tyr160, Ala161, Val203, Ser205, Ser206, Thr207, Tyr210, and Val212 of human α1 subunit. Phe127, Tyr187, and Tyr237 of α2 interact with the diazepine ring and Thr142 of ɣ subunit mediated an H-bond with the carbonyl group of flumazenil. Moreover, flumazenil also formed H-bonds with His102(ɣ), His129(α2), Ser232(α2), Tyr187(α2), and π-π interactions with Tyr237(α2). At the α2-β3 interface, flumazenil interacts with Asn41 and Gln64 of β3 through hydrophobic contacts. Another modulator, pregnenolone sulfate (PS) binds between the M3-M4 region of α1 and α2 subunits mainly through hydrophobic interactions. The residues of α1 (Phe295, Ser298, Glu302, Arg316, Lys390, Ile391, Leu394, Ser395, Ala398, Phe399, and Leu402) were identical to Phe323, Ser326, Glu330, Thr333, Phe337, Ser413, Ile417, Met420, Ser421, Val424, and Phe425, are Leu428 of α2 model. The Arg316 of α1 interact with the sulfate group of the compound through an H-bond. However, human α2 possesses serine residue instead of arginine which does not offer H-bond to PS at this site. Alphaxalone (ALP) and tetrahydro deoxy corticosterone

(THDOC) binds at the region between TM1(α) and TM3 (β) at α1-β2, α1-β3, and α2-β2 complexes. ALP mediates hydrophobic interaction with Trp273 and Tyr304 and H-bonding with Gln269 of α2. In the α1 subunit, ALP formed H-bond with Thr306 which is replaced by Leu in α2, which does not offer H-bond to ALP. At the β3 subunit, Phe301 and Tyr304 (located at M3) stabilize the substituted –OH and carbonyl moieties of THDOC via hydrophobic interactions.

We have docked the compound, 2'-Cl-6-MF at all the predicted binding sites in α2β2γ2L and α2β3γ2L complexes. The docking results indicated that 2'-Cl-6-MF favorably binds at BZD binding region located at α2-γ2 interface in α2β2γ2L complex, where flavone oxygens interact with the side chain –OH of Ser323(α2) and OH of Thr142(γ2) at a distance of 1.92 Å and 2.57 Å, respectively. The methyl-substituted phenyl ring of the compound is located at the ECD region of α2 where the side chains of Tyr237, His129, Ala188, Tyr187, and Phe127 stabilize the compound through hydrophobic interactions. The chlorophenyl moiety of the compound is oriented towards the ECD region of γ2 subunit where several residues including Tyr58, Glu189, Asp56, Ala79, Phe77, Thr142, and Met130 provides hydrophobic interactions to the compound. The compound did not show favorable binding interaction at the GABA binding site, which is also evident from its docking score (+2.85). The docking score of the compound at the α2-γ2 interface is − 6.50 which is greater than the binding scores of 2'-Cl-6MF at M1(α2)-M3(β2) region (− 4.74) and M3-M4(α2) region (− 4.10). Furthermore, the compound was found to be surface-exposed when docked at the transmembrane regions. The docking scores indicate that the compound preferentially binds at the α2-γ2 interface. The docked view of the compound at the α2-γ2 interface is shown in Fig. 7a. Similarly, when docked at different predicted pockets of α2β3γ2L complex, the compound showed significant binding at the α2-γ2 interface as compared to the α2-β3 interface and transmembrane regions of α2 and β3 subunit. The main chain amino group and the side chain –OH of Ser233 of α2 subunit provides bidentate interactions to the flavone oxygen of the compound in α2β3γ2L complex. The docked view of the compound at GABA binding site at the α2-β3 interface suggests that the compound may interact with the amino and the –OH groups of Thr202 of the β3 subunit, however, the docking score at this site (− 2.17) is very low as compared to the other sites. The docking score of the compound at an α2-γ2 interface (BZD binding site) was − 9.87, which was significantly higher than the docking score of

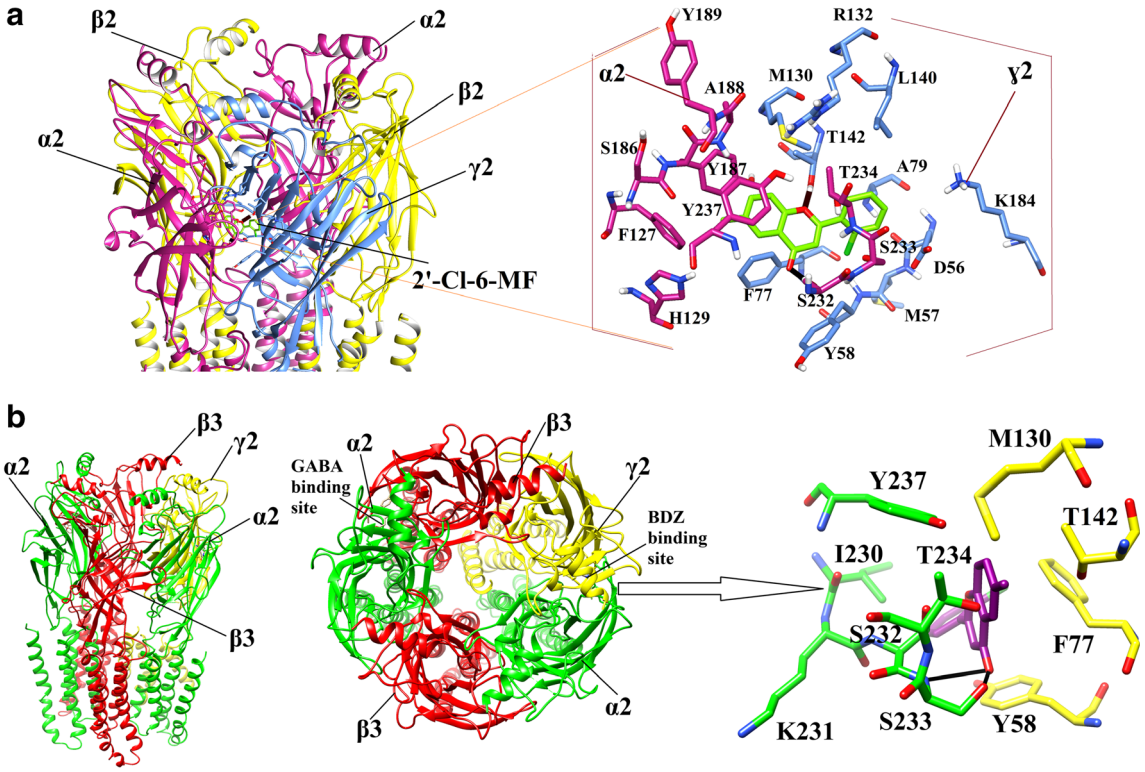

Fig. 7 **a** The extracellular domain of the α2β2γ2L complex is shown. The α2, β2, and γ2 subunits are shown in hot pink, yellow, and blue colors, respectively. The binding mode of 2'-Cl-6MF at the α2-γ2 interface is highlighted. The ligand is shown in the green stick model, binding residues of α2 and γ2 are depicted in hot pink and blue stick models, respectively. Hydrogen bonds are shown in black lines. **b** The 3D-structure of the α2β3γ2L complex is shown. The α2, β3, and γ2 subunits are shown in green, red, and yellow colors, respectively. The top view of ECD region of α2β3γ2L is presented to show the binding regions. The binding mode of 2'-Cl-6MF at the α2-γ2 interface is highlighted. The ligand is shown in the magenta stick model, binding residues of α2 and γ2 are depicted in the green and yellow stick model, respectively. Hydrogen bonds are shown in black lines

the compound at other predicted binding sites. The binding interactions of the compound are shown in Fig. 7b. The docking results suggest that the compound has preferential binding potential towards the α2-γ2 interface in both the complexes.

Discussion

Cisplatin is used in chemotherapy in the treatment of various types of cancers including lung, ovarian, and breast cancers (van der Burg et al. 2002; Woods et al. 1990). Several pathophysiological mechanisms including increased ion channel expression and activity are implicated in the pathophysiology of cisplatin-induced neuropathic pain (Quintão et al. 2019). Reduced GABAergic or glycinergic inhibition in the spinal dorsal horn (i.e., in the sensory part of the spinal cord) is implicated in chronic pain syndromes (Coull et al. 2003; Harvey et al. 2004; Zeilhofer 2008). BDZ-sensitive GABA-A receptors include either α1, α2, α3, or α5, together with a β subunit and a γ2 subunit in a stoichiometric ratio of 2:2:1 (Barnard 2001). Of special interest are α2- and α3-GABA-A subtypes selective agonists which are effective in treating chronic neuropathic pain. For example, HZ166 with preferential α2 and α3 subtype selectivity was found to possess antihyperalgesic effects in chronic constriction injury (CCI) of the sciatic nerve in mice (Di Lio et al. 2011).

We have previously shown flavonoids differentially modulate GABA-A receptors (Karim et al. 2011). They have enhanced efficacy at α2-containing GABA-A receptors (Karim et al. 2011). Thus, in the present study, we investigated 2'-Cl-6MF for their effects on recombinant α1, α2, and α3 subtypes containing GABA-A receptors expressed in *Xenopus* oocytes. We found that 2'-Cl-6MF selectively potentiated GABA-elicited α2β2/3γ2L and α3β2/3γ2L GABA-A receptor subtypes. 2'-Cl-6MF also did not cause any enhancement of GABA-induced current at α1β2γ2L subtype. Furthermore, flumazenil blocked the potentiation induced by 2'-Cl-6MF at indicating the involvement of classical high-affinity benzodiazepine site in its potentiation of GABA effect. This is in contrast to findings obtained with 2'-MeO6MF (Karim et al. 2012) and 3-OH-2'-MeO6MF (Karim et al. 2011) where flumazenil failed to block both GABA potentiation at selected GABA-A receptor subtypes and α2β2γ2L GABA-A receptor subtype anxiolytic effects in mice. It appears that the halogen substitution for the methoxy group at the 2' position of ring C confers benzodiazepine sensitivity to this compound.

Next, we evaluated the effects of 2'-Cl-6MF on mechanical allodynia in the Von Frey test. The results showed that 2'-Cl-6MF (10–100 mg/kg) exerted a significant antiallodynic effect as it reversed decreases in paw withdrawal threshold caused by cisplatin. To assess the involvement of GABA-A receptors, pretreatment of animals with PTZ reversed the enhancement of paw withdrawal threshold by 2'-Cl-6MF indicating that antiallodynic effects of 2'-Cl-6MF possibly involve α2β2/3γ2L GABA-A receptor subtypes. The involvement of BDZ in the antinociceptive effect of 2'-Cl-6MF was also evaluated using flumazenil and the results showed amelioration of the antiallodynic effects of 2'-Cl-6MF. The results of electrophysiological and behavioral studies indicate that 2'-Cl-6MF exhibit a profile which is matched by most flavonoids which mediate their pharmacological effects via the BDZ site of GABA-A receptors. For example, 6-chloroflavone, 6-fluoroflavone, 6-bromoflavone, 6-hydroxyflavone, and 6,20-dihydroxyflavone demonstrated to be a positive modulator at GABA-A receptors acting via flumazenil-sensitive high-affinity classical benzodiazepine sites (Hanrahan et al. 2015; Ren et al. 2010).

The antiallodynic effects of 2'-Cl-6MF were found to be comparable with gabapentin (GBP). Gabapentin is used clinically in the treatment of diabetes and chemotherapy-induced neuropathic pain (Jensen et al. 2009). However, its antihyperalgesic effects are accompanied by adverse effects including sedation dizziness, motor incoordination, and ataxia. This may be due to complex mechanisms of gabapentin including activating the heterodimeric GABAB receptors and enhancing the NMDA current at GABAergic interneurons. It may also block AMPA-receptor–mediated transmission in the spinal cord, and activate ATP-sensitive K+ channels. The antinociceptive effects of gabapentin may be mediated via the 2δ subunit of spinal N-type Ca2+ channels (Cheng and Chiou 2006). Our results are consistent with these findings where PTZ failed to block the antinociceptive effects of gabapentin in the Von Frey test.

The findings that cisplatin does not appear to cause thermal allodynia are consistent with previous studies wherein no significant change either in cold or heat allodynia has been found with an intraplantar injection of cisplatin (Park et al. 2013; Ta et al. 2009). This was believed to be due to the accumulation of high local concentrations of cisplatin at the sensory nerve endings as a result of the intraplantar injection. This high concentration is achieved via accumulation of the cisplatin in the sensory nerve endings through copper transporters and thus results in the development of sensory neuropathy (Liu et al. 2013). Intraplantar injection of platinum-based chemotherapeutics agents directly exposes peripheral sensory nerve endings to the high local concentration of cisplatin (Lancaster et al. 2013; Sprowl et al. 2013) reflecting the accumulation that results from intravenous administration in clinical settings. Thus, this model accurately reflects the clinical presentation of cisplatin-induced neuropathy wherein mechanical allodynia is present, but cold and heat allodynia are absent (Deuis et al. 2014).

Flavonoids have been shown to traverse the blood brain barrier (BBB) and are able to localize in specific brain areas, suggesting that they are potential candidates for

neuromodulatory effects. For example, we have previously shown that the pharmacokinetic studies of 6-methoxyflavone indicated that it not only crosses BBB but can also achieve considerable concentration in various brain areas including brain stem and cerebral cortex involved in the modulation of neuropathic pain (Akbar et al. 2017).

Computational modeling has been used extensively to determine the three-dimensional structures of proteins of interest, hit finding, and lead optimization (Prieto-Martínez et al. 2019). In silico techniques have played a crucial role in the discovery of drug-like-compounds that are currently in clinical use, for example, several molecules have been identified for the treatment of glaucoma, nonsmall-cell lung cancer, influenza virus infections, and acquired immunodeficiency syndrome using computer-aided drug design (CADD) approaches. CADD is segregated in the structure-based (SBDD) and the ligand-based drug design (LBDD) methods that use the structural information of the protein and ligands, respectively. Herein, we have applied SBDD methods including homology modeling and molecular docking which are used for the prediction of the structures of protein and their binding with the inhibitors, respectively. Using homology modeling tools, the coordinates of the α2 subtype was generated and inserted into α2β2γ2L and α2β3γ2L complexes. Later, the binding of 2'-Cl-6MF within these complexes was studied by docking which demonstrated that 2'-Cl-6MF may target the neuromodulator binding site of the receptors. The binding site of $GABA_A$α2 subunit was compared with the binding sites of $GABA_A$α1 and $GABA_A$α3 subunits by sequence and structural alignment. Most of the binding residues in α2 subunit (Phe127, His129, Lys183, Ser186, Tyr187, Ala188, Tyr189, Thr190, Ser232. Ser233, Thr234, Gly235, and Tyr237) were completely identical in all three subunits (Table S3, supporting information). However, Thr199 (α2) and Thr216 (α3) are replaced with Arg164 in α1 subunit. Moreover, Ser192 of α2 is replaced with Ala in α1 and α3. While Glu228(α2) and Glu253(α3) are replaced with Gly residue in α1, similarly, Thr229 of α2 subunit is replaced with Ile moiety in both α1 and α3 subunit. More interestingly, Ile230 of α2 and Ile255 of α3 are changed with Val203 in α1 subunit. This Ile230(α2) play important role in the stabilization of chlorophenyl ring of 2'-Cl-6MF through hydrophobic interactions. Due to the smaller side chain of Val and high conformational flexibility of α1 subunit, Val residue found to be located far from the compounds, and the hydrophobic interaction was lost at this positon. The aligned view of these subunits are shown in Fig. S3 in supporting information.

To the best of our knowledge, this is the first study that evaluates the antiallodynic effect of a novel synthetic flavone, 2'-Cl-6MF on mechanical allodynia caused by cisplatin. Furthermore, the antiallodynic effects of 2'-Cl-6MF are most likely mediated via classical benzodiazepine sites of α2 and/or α3-containing GABA-A receptors. Thus, 2'-Cl-6MF may provide a lead for the development of safe and effective agents for treating chronic neuropathic pain caused by cisplatin.

Supplementary Information The online version contains supplementary material available at https://doi.org/10.1007/s00210-020-02021-x.

Acknowledgments Dr. Nasiara Karim acknowledges funding (National research program for universities; NRPU 20-3425) from the Higher Education Commission of Pakistan for the completion of this research work. The funding body did not contribute to the design or any other part of the research work. We also acknowledge Professor Dr. Mary Collins, faculty of Pharmacy, the University of Sydney for providing technical assistance in oocytes experiments.

Authors' contribution NK, AK, NA, and IK performed the in vivo experiments. AA synthesized the compound. AK, AAH, and RK characterized the compound. SAH performed the molecular docking. NK, AK, WA, and SAH wrote and refined the manuscript. All authors read and approved the manuscript, and all data were generated in-house and that no paper mill was used.

References

Akbar S, Subhan F, Karim N, Aman U, Ullah S, Shahid M, Ahmad N, Fawad K, Sewell RDE (2017) Characterization of 6-methoxyflavanone as a novel anxiolytic agent: a behavioral and pharmacokinetic approach. Eur J Pharmacol 801:19–27

Barnard EA (2001) The molecular architecture of GABA-A receptors. In: pharmacology of GABA and Glycine neurotransmission. In: Möhler HE (ed) The molecular architecture of GABA-A receptors. Springer, Berlin, p 2001

Bouhassira D, Lanteri-Minet M, Attal N, Laurent B, Touboul C (2008) Prevalence of chronic pain with neuropathic characteristics in the general population. Pain 136:380–387

Cheng J-K, Chiou L-C (2006) Mechanisms of the Antinociceptive action of gabapentin. J Pharmacol Sci 100:471–486

Coull JA, Boudreau D, Bachand K, Prescott SA, Nault F, Sik A et al (2003) Trans-synaptic shift in anion gradient in spinal lamina I neurons as a mechanism of neuropathic pain. Nature. 424:938–942

Deng L, Guindon J, Vemuri VK, Thakur GA, White FA, Makriyannis A et al (2012) The maintenance of cisplatin- and paclitaxel-induced mechanical and cold allodynia is suppressed by cannabinoid CB(2) receptor activation and independent of CXCR4 signaling in models of chemotherapy-induced peripheral neuropathy. Mol Pain 8:71

Deuis JR, Lim YL, Rodrigues de Sousa S, Lewis RJ, Alewood PF, Cabot PJ et al (2014) Analgesic effects of clinically used compounds in novel mouse models of polyneuropathy induced by oxaliplatin and cisplatin. Neuro-oncology 16:1324–1332

Di Lio A, Benke D, Besson M, Desmeules J, Daali Y, Wang ZJ et al (2011) HZ166, a novel GABAA receptor subtype-selective benzodiazepine site ligand, is antihyperalgesic in mouse models of inflammatory and neuropathic pain. Neuropharmacology. 60:626–632

Gregg RW, Molepo JM, Monpetit VJ, Mikael NZ, Redmond D, Gadia M, Stewart DJ (1992) Cisplatin neurotoxicity: the relationship between dosage, time, and platinum concentration in neurologic tissues, and morphologic evidence of toxicity. J Clin Oncol 10:795–803

Hanrahan JR, Chebib M, Johnston GA (2015) Interactions of flavonoids with ionotropic GABA receptors. Adv Pharmacol 72:189–200

Harvey RJ, Depner UB, Wassle H, Ahmadi S, Heindl C, Reinold H et al (2004) GlyR alpha3: an essential target for spinal PGE2-mediated inflammatory pain sensitization. Science. 304:884–887

Jensen TS, Madsen CS, Finnerup NB (2009) Pharmacology and treatment of neuropathic pains. Curr Opin Neurol 22:467–474

Karim N, Gavande N, Wellendorph P, Johnston GA, Hanrahan JR, Chebib M (2011) 3-Hydroxy-2′-methoxy-6-methylflavone: a potent anxiolytic with a unique selectivity profile at GABA(A) receptor subtypes. Biochem Pharmacol 82:1971–1983

Karim N, Curmi J, Gavande N, Johnston GA, Hanrahan JR, Tierney ML et al (2012) 2′-Methoxy-6-methylflavone: a novel anxiolytic and sedative with subtype selective activating and modulating actions at GABA(A) receptors. Br J Pharmacol 165:880–896

Knabl J, Witschi R, Hosl K, Reinold H, Zeilhofer UB, Ahmadi S et al (2008) Reversal of pathological pain through specific spinal GABAA receptor subtypes. Nature. 451:330–334

Knabl J, Zeilhofer UB, Crestani F, Rudolph U, Zeilhofer HU (2009) Genuine antihyperalgesia by systemic diazepam revealed by experiments in GABAA receptor point-mutated mice. Pain. 141:233–238

Krarup-Hansen A, Fugleholm K, Helweg-Larsen S, Hauge EN, Schmalbruch H, Trojaborg W, Krarup C (1993) Examination of distal involvement in cisplatin-induced neuropathy in man. An electrophysiological and histological study with particular reference to touch receptor function. Brain. 116(Pt 5):1017–1041

Lancaster CS, Sprowl JA, Walker AL, Hu S, Gibson AA, Sparreboom A (2013) Modulation of OATP1B-type transporter function alters cellular uptake and disposition of platinum chemotherapeutics. Mol Cancer Ther 12:1537–1544

Liu JJ, Kim Y, Yan F, Ding Q, Ip V, Jong NN, Mercer JFB, McKeage MJ (2013) Contributions of rat Ctr1 to the uptake and toxicity of copper and platinum anticancer drugs in dorsal root ganglion neurons. Biochem Pharmacol 85:207–215

Miri A, Sharifi-Rad J, Tabrizian K, Nasiri AA (2015) Antinociceptive and anti-inflammatory activities of *Teucrium persicum* Boiss. Extract Mice Sci 2015:972827

Olsen RW, Sieghart W (2008) International Union of Pharmacology. LXX. Subtypes of gamma-aminobutyric acid(A) receptors: classification on the basis of subunit composition, pharmacology, and function. Update. Pharmacol Rev 60:243–260

Park HJ (2014) Chemotherapy induced peripheral neuropathic pain. Korean J Anesthesiol 67:4–7

Park HJ, Stokes JA, Pirie E, Skahen J, Shtaerman Y, Yaksh TL (2013) Persistent hyperalgesia in the cisplatin-treated mouse as defined by threshold measures, the conditioned place preference paradigm, and changes in dorsal root ganglia activated transcription factor 3: the effects of gabapentin, ketorolac, and etanercept. Anesth Analg 116:224–231

Prieto-Martínez FD, López-López E, Juárez-Mercado KE, Medina-Franco JL (2019) Computational drug design methods—current and future perspectives. In silico drug design: Elsevier. p. 19–44

Quintão NLM, Santin JR, Stoeberl LC, Corrêa TP, Melato J, Costa R (2019) Pharmacological treatment of chemotherapy-induced neuropathic pain: PPARγ agonists as a promising tool. Front Neurosci 13

Rahn EJ, Zvonok AM, Thakur GA, Khanolkar AD, Makriyannis A, Hohmann AG (2008) Selective activation of cannabinoid CB2 receptors suppresses neuropathic nociception induced by treatment with the chemotherapeutic agent paclitaxel in rats. J Pharmacol Exp Ther 327:584–591

Ren L, Wang F, Xu Z, Chan WM, Zhao C, Xue H (2010) GABAA receptor subtype selectivity underlying anxiolytic effect of 6-hydroxyflavone. Biochem Pharmacol 79:1337–1344

Roelofs RI, Hrushesky W, Rogin J, Rosenberg L (1984) Peripheral sensory neuropathy and cisplatin chemotherapy. Neurology. 34:934–938

Rudolph U, Crestani F, Benke D, Brunig I, Benson JA, Fritschy JM et al (1999) Benzodiazepine actions mediated by specific gamma-aminobutyric acid(A) receptor subtypes. Nature. 401:796–800

Sang CS, Hayes KS (2006) Anticonvulsant medications in neuropathic pain. In: McMahon SB, K. M, (eds) Wall and Melzack's Textbook of Pain. Elsevier

Smith EML, Pang H, Cirrincione C, Fleishman S, Paskett ED, Ahles T, Bressler LR, Fadul CE, Knox C, le-Lindqwister N, Gilman PB, Shapiro CL, Alliance for Clinical Trials in Oncology (2013) Effect of duloxetine on pain, function, and quality of life among patients with chemotherapy-induced painful peripheral neuropathy: a randomized clinical trial. J Am Med Assoc 309:1359–1367

Sprowl JA, Ciarimboli G, Lancaster CS, Giovinazzo H, Gibson AA, Du G et al (2013) Oxaliplatin-induced neurotoxicity is dependent on the organic cation transporter OCT2. Proc Natl Acad Sci U S A 110:11199–11204

Ta LE, Low PA, Windebank AJ (2009) Mice with cisplatin and oxaliplatin-induced painful neuropathy develop distinct early responses to thermal stimuli. Mol Pain 5:9

Thompson SW, Davis LE, Kornfeld M, Hilgers RD, Standefer JC (1984) Cisplatin neuropathy. Clinical, electrophysiologic, morphologic, and toxicologic studies. Cancer. 54:1269–1275

van der Burg ME, de Wit R, van Putten WL, Logmans A, Kruit WH, Stoter G et al (2002) Weekly cisplatin and daily oral etoposide is highly effective in platinum pretreated ovarian cancer. Br J Cancer 86:19–25

Woods RL, Williams CJ, Levi J, Page J, Bell D, Byrne M, Kerestes ZL (1990) A randomised trial of cisplatin and vindesine versus supportive care only in advanced non-small cell lung cancer. Br J Cancer 61:608–611

Zeilhofer HU (2008) Loss of glycinergic and GABAergic inhibition in chronic pain–contributions of inflammation and microglia. Int Immunopharmacol 8:182–187